# Impact of $CO_2$-Induced Warming on Simulated Hurricane Intensity and Precipitation: Sensitivity to the Choice of Climate Model and Convective Parameterization

THOMAS R. KNUTSON

*NOAA/Geophysical Fluid Dynamics Laboratory, Princeton, New Jersey*

ROBERT E. TULEYA

*Center for Coastal Physical Oceanography, Old Dominion University, Norfolk, Virginia*

(Manuscript received 12 December 2003, in final form 24 March 2004)

ABSTRACT

Previous studies have found that idealized hurricanes, simulated under warmer, high-$CO_2$ conditions, are more intense and have higher precipitation rates than under present-day conditions. The present study explores the sensitivity of this result to the choice of climate model used to define the $CO_2$-warmed environment and to the choice of convective parameterization used in the nested regional model that simulates the hurricanes. Approximately 1300 five-day idealized simulations are performed using a higher-resolution version of the GFDL hurricane prediction system (grid spacing as fine as 9 km, with 42 levels). All storms were embedded in a uniform 5 m $s^{-1}$ easterly background flow. The large-scale thermodynamic boundary conditions for the experiments—atmospheric temperature and moisture profiles and SSTs—are derived from nine different Coupled Model Intercomparison Project (CMIP2+) climate models. The $CO_2$-induced SST changes from the global climate models, based on 80-yr linear trends from +1% $yr^{-1}$ $CO_2$ increase experiments, range from about +0.8° to +2.4°C in the three tropical storm basins studied. Four different moist convection parameterizations are tested in the hurricane model, including the use of no convective parameterization in the highest resolution inner grid. Nearly all combinations of climate model boundary conditions and hurricane model convection schemes show a $CO_2$-induced increase in both storm intensity and near-storm precipitation rates. The aggregate results, averaged across all experiments, indicate a 14% increase in central pressure fall, a 6% increase in maximum surface wind speed, and an 18% increase in average precipitation rate within 100 km of the storm center. The fractional change in precipitation is more sensitive to the choice of convective parameterization than is the fractional change of intensity. Current hurricane potential intensity theories, applied to the climate model environments, yield an average increase of intensity (pressure fall) of 8% (Emanuel) to 16% (Holland) for the high-$CO_2$ environments. Convective available potential energy (CAPE) is 21% higher on average in the high-$CO_2$ environments. One implication of the results is that if the frequency of tropical cyclones remains the same over the coming century, a greenhouse gas–induced warming may lead to a gradually increasing risk in the occurrence of highly destructive category-5 storms.

## 1. Introduction

Emanuel (1987) used a theoretical model of tropical cyclone potential intensity to propose that tropical cyclones in a greenhouse gas–warmed climate would have higher potential intensities than in the present-day climate. This scenario has received some support from Holland's (1997) alternative potential intensity theory (Tonkin et al. 1997; Henderson-Sellers et al. 1998) as well as from three-dimensional hurricane modeling studies using regional nested modeling approaches (Knutson et al. 1998; Knutson and Tuleya 1999; Walsh and Ryan 2000; Knutson et al. 2001), although several caveats have been noted, for example, by Henderson-Sellers et al. (1998).

One limitation of the nested model-based approaches of Knutson et al. (2001) and Knutson and Tuleya (1999) has been that the tropical climate states (present day and high $CO_2$) used as input to the hurricane model simulations have been derived from a single global climate model—the Geophysical Fluid Dynamics Laboratory (GFDL) R30 coupled model. Also a single version of the GFDL hurricane model has been used to simulate the hurricane behavior. In this report, these particular limitations are relaxed through a series of sensitivity experiments. For example, climate change scenarios from nine different global coupled climate models are used as inputs to the idealized hurricane model. These model scenarios have been made available by various institutions (Table 1) as part of the Coupled Model In-

*Corresponding author address:* Thomas R. Knutson, NOAA/Geophysical Fluid Dynamics Laboratory, P.O. Box 308, Forrestal Campus, U. S. Rte. 1, Princeton, NJ 08542.
E-mail: Tom.Knutson@noaa.gov

TABLE 1. CMIP2+ models used in the present study and their developing institutions.

| Model | Developer |
|---|---|
| CCCma (CGCM2) | Canadian Centre for Climate Modelling and Analysis (CCCma), Canada |
| CSIRO (Mk2) | CSIRO, Australia |
| CSM1 | NCAR-led consortium, United States |
| ECHAM4/OPYC3 | Max Plank Institute, Germany |
| GFDL (R30) | NOAA/GFDL, United States |
| HadCM2 | Met Office, United Kingdom |
| HadCM3 | Met Office, United Kingdom |
| MRI (CGCM2.3) | MRI, Japan |
| PCM | NCAR and Department of Energy, United States |

tercomparison Project (CMIP2+). Hurricane simulations are known to be sensitive to parameterizations of moist physics. Sensitivity tests are therefore performed with four different versions of cumulus convection parameterization in the hurricane model. In addition, the effect of spatial resolution is evaluated by the use of a higher-resolution version of the hurricane model (grid spacing as fine as 9 km, with 42 vertical levels, as opposed to the 18 km/18 vertical-level model used in the previous studies).

In the present study, no ocean coupling beneath the storm is used in the hurricane model even though it is now well established that such ocean coupling can have a substantial impact on hurricane intensity (e.g., Ginis 1995; Schade and Emanuel 1999; Bender and Ginis 2000). The use of an uncoupled model is justified for the present study, since Knutson et al. (2001) demonstrated that a similar percentage increase in hurricane intensity was simulated for high-$CO_2$ conditions for both coupled and uncoupled models.

An important limitation of the present study is that it does not address the question of possible changes in tropical cyclone frequency in a warmer climate. Some attempts have been made to address this question by examining the occurrence of tropical storm–like vortices in global climate models (Broccoli and Manabe 1990; Haarsma et al. 1993; Bengtsson et al. 1996; Krishnamurti et al. 1998; Sugi et al. 2002; Tsutsui 2002) or in a nested regional model (Nguyen and Walsh 2001). Royer et al. (1998) used a modified form of Gray's (1975) genesis parameters in which they attempted to address climate change issues noted by Ryan et al. (1992). These studies give conflicting results, even with regard to the sign of the change in frequency with greenhouse warming, and the results are still regarded as inconclusive (Henderson-Sellers et al. 1998; Giorgi et al. 2001). Another limitation of our study is the neglect of dynamical influences, such as vertical wind shear, on the storms in our idealized setting. This issue is discussed in more detail in section 5.

The remainder of this paper is organized as follows: In section 2, the methodology of the idealized hurricane experiments is described. The climate change scenarios from the nine CMIP2+ models are summarized in section 3. In section 4, results of the sensitivity experiments are presented along with an analysis of the statistical associations between the simulated hurricane intensities (or precipitation) and various environment measures. Section 5 discusses the possible role of vertical wind shear, and section 6 contains concluding remarks.

## 2. Methodology for the idealized hurricane simulations

### *a. Hurricane model overview*

The hurricane simulations in this study use the idealized framework described in Shen et al. (2000) and Knutson and Tuleya (1999). Briefly, for each of the idealized experiments, a hurricane is simulated in a regional model using highly idealized boundary forcing and initial conditions. The large-scale environment consists of a uniform easterly flow (5 m $s^{-1}$) with no vertical or horizontal shear above the boundary layer. The SST over the entire domain and the vertical profiles of temperature and moisture at the lateral boundaries (and in the interior at the initial time) are specified based on time mean SST and profiles from global climate models. A robust initial hurricane disturbance is inserted into this background environment, as described in section 2c, and allowed to evolve for 5 days.

An updated higher-resolution version of the GFDL Hurricane Prediction System (Kurihara et al. 1998) is used. Although closely related to the system used operationally for hurricane prediction at the National Centers for Environmental Prediction (NCEP) in 2003, the model used for the current study is an enhanced horizontal resolution version consisting of a 42-level, triply nested moveable-mesh atmospheric model with the Mellor–Yamada 2.5 boundary layer formulation. The outer/medium/inner mesh covers a 75° × 75°/11° × 11°/5° × 5° region with a grid spacing of $1/2°/1/6°/1/12°$, or about 54/18/9 km. The high-resolution meshes in the model move with the storm in order to concentrate resolution around it to better resolve some important features of the hurricane such as the eye. Other details of the model are contained in Kurihara et al. (1998) and references therein.

### *b. Convective parameterizations tested*

Four methods of convective parameterization are available in the current version of the GFDL hurricane

model and are tested in our sensitivity analysis. The four types include two mass flux schemes, a convective adjustment scheme, and resolved convection (i.e., using no convective parameterization). The PAN scheme refers to the simplified Arakawa–Schubert (SAS) mass flux scheme as implemented by Pan and Wu (1995) and Hong and Pan (1996) in the current global forecast system (GFS) at NCEP. The PAN scheme is also used in the current operational version (2003 hurricane season) of the GFDL hurricane model. The EMAN scheme refers to the mass flux scheme developed by Emanuel (1991) and Emanuel and Živković-Rothman (1999), as implemented in the U.S. Navy Operational Global Atmospheric Prediction System (NOGAPS; Peng et al. 2003, personal communication). KURI will refer to the ''soft convective adjustment'' scheme used in operational versions of the GFDL hurricane model (Kurihara et al. 1998) prior to the 2003 hurricane season. For the resolved convection cases, the model was integrated with no cumulus convective parameterization in the innermost (1/12°) grid. Rainfall is then assumed to occur if a state of supersaturation occurs in the model. For simplification, no cloud microphysical packages are invoked. For the resolved convection cases, the EMAN convective parameterization scheme was used outside the highest-resolution mesh due to the much coarser horizontal resolution. Although even the innermost grid, with 9-km grid spacing, has quite a coarse resolution for a model without convective parameterization, we have performed a series of such sensitivity experiments here to give an initial indication of the behavior that may result as resolution is further increased and no convective parameterization is used.

To illustrate the effect that altering the convection parameterization has on the hurricane simulations, Fig. 1 shows the instantaneous precipitation rate (cm day$^{-1}$) at simulation hour 120 for one of the idealized hurricane cases. Figures 1a–d differ only in the type of convective parameterization used. All of the cases show a well-developed hurricane with a circular core of strong precipitation surrounding a local minimum—the model's representation of the hurricane eye. The core region of strongest precipitation is largest for the Pan convection scheme (Fig. 1c) and smallest for the resolved convection and Kurihara runs (Figs. 1b,d). Although there is no ''ground truth'' for these simulations, it appears to us that the rainband and inner-core features for the Emanuel and Pan schemes are more realistic than those for the resolved convection and Kurihara cases. The Kurihara scheme in this case study shows the weakest outer rainband features, although our experience has been that this scheme produces more pronounced rainbands in experiments using less idealized environmental flow fields.

In the resolved convection case (Fig. 1b), some discontinuities appear at the boundary between the innermost mesh and the outer meshes. These discontinuities are marked by meridionally oriented ''lines'' of precipitation along 88°–89°W and a precipitation deficit just inside the boundary of the 5° × 5° innermost grid centered on the storm. We note that in addition to enhanced resolution, the innermost mesh in Fig. 1b differs from the outer meshes in terms of the physical model being used. Emanuel convection is used in the outer meshes, while only resolved convection (no parameterization of subgrid-scale convection) is used in the innermost mesh. This change in the physical model between these regions is probably responsible for some of the spurious precipitation features in Fig. 1b such as the precipitation deficit occurring just inside the boundary of the inner grid.

In Figs. 1a–d, the outer meshes of the domains contain larger-scale precipitation features than does the innermost grid. The largest features are in the lowest resolution (1/2° grid spacing) outer grid, which extends over a 75° × 75° region. (Note that this is a considerably larger domain than shown in Fig. 1.) These large-scale precipitation features are an artifact of the limited resolution in these regions and point to the limitations of the nested modeling approach. Future increases of computing power will enable simulation studies of increasingly large domains with a resolution as fine as that used here for the innermost grid, for example.

In summary, the results in Fig. 1 indicate that the convective parameterization can have an important impact on the structure of the simulated hurricanes. Furthermore the explicitly resolved convection case yields a reasonable simulated hurricane, to first order, despite the rather coarse resolution (~9-km grid spacing) and other simulation deficiencies noted for this approach.

### *c. Initialization procedure*

In this section, the method used to initialize the hurricane test cases is described. The SST and atmospheric temperature and moisture profiles for the experiments are derived from time-mean climatologies from the global climate models as described in section 3. To create the initial storm condition, an initial disturbance is generated by nudging an axisymmetric version of the hurricane model toward a specified target wind profile (Kurihara et al. 1998), beginning from a state of rest with the initial temperature and moisture profiles derived from a global climate model tropical basin mean state. The target disturbance is based on a real hurricane case (Hurricane Fran, 2 September 1996) and has maximum surface wind speeds of approximately 35 m s$^{-1}$ at a radius of 55 km. The resulting disturbance vortex is superimposed on the environmental flow to create the total initial wind distribution for the full three-dimensional model. The surface pressure and the temperature fields over the model domain are then computed by solving a form of the reverse balance equation (Kurihara et al. 1993), using the climate model-derived temperatures as a reference boundary condition at the latitude where the storm is inserted. The resulting SST, tem-

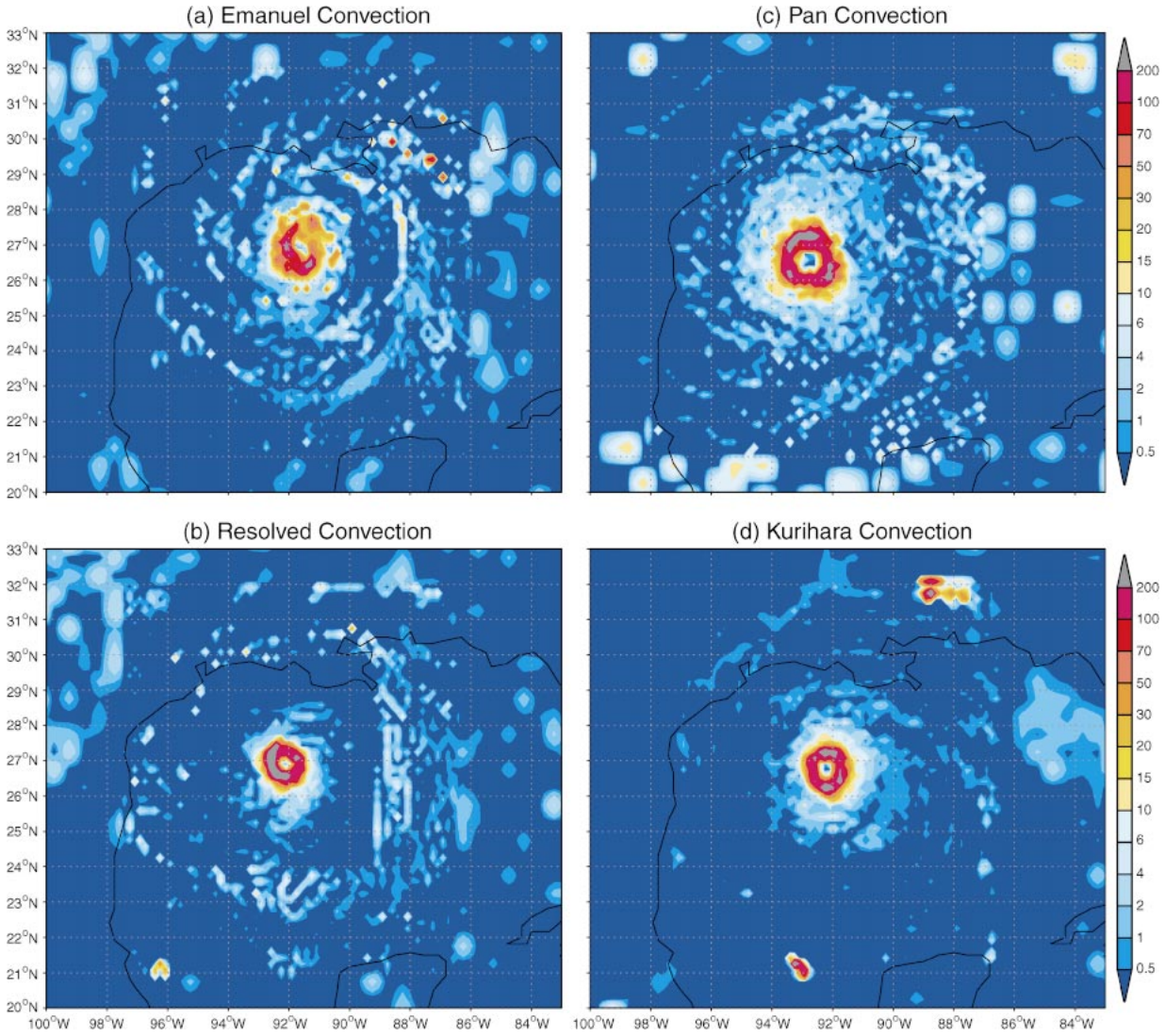


FIG. 1. Instantaneous precipitation rates (cm day$^{-1}$) at simulation hour 120 for sample idealized hurricane experiments using the following convection treatments: (a) Emanuel convection, (b) resolved inner-nest convection with Emanuel convection in the outer two nests, (c) Pan convection, and (d) Kurihara convection. The boundary/initial environmental conditions for the runs are derived from the HadCM3 control run for the NW Pacific basin. The U.S. Gulf Coast geography is included for scale only; no land is included in the simulations. See text for further details.

perature, and moisture fields outside the storm disturbance region are approximately horizontally uniform and closely approximate the original profiles derived from the climate models. The initial storm disturbance is an anomaly from those conditions that is designed to be compatible with the hurricane model physics. Each storm in this study was embedded in a uniform 5 m s$^{-1}$ easterly environmental flow. The use of such an idealized environmental flow precludes any influence of vertical wind shear or other dynamical environmental flow features on the results, a topic that we will return to in section 5. A relatively strong target initial intensity was chosen to assure strong development among all model initial conditions and all convective parameterizations.

The same initial target wind profile is used for each experiment in this study, except for small random perturbations to the specified maximum intensity of the vortex. Specifically, an ensemble of six experiments, each developed as a small perturbation from the ''base case'' initial target, is used to create an ensemble of closely related, but not identical, initial conditions for each set of climate model boundary conditions. This ensemble approach is used to evaluate the robustness of our results to small variations in initial conditions. The sample of randomly perturbed initial target maximum intensities is derived from a Gaussian distribution with a mean of 35 m s$^{-1}$ and standard deviation of 0.5 m s$^{-1}$. The resulting average initial intensity is 971 mb in terms of central pressure, with a range of initial in-

tensities of approximately 967–976 mb for the ensemble members.

The global models used in this study all differ from the regional hurricane model in terms of spatial resolution, model physics, etc. These model differences can be expected to lead to differences between the hurricane model and global model climatologies. Even during the relatively short 5-day integrations used here, the atmospheric fields away from the lateral boundaries in the hurricane model will tend to adjust toward the hurricane model's climatology (except for SST, which is held constant in time). Since these atmospheric adjustments occur in both the control and high-$CO_2$ experiments, it is assumed that their net effect on the sensitivity results (high $CO_2$ minus control) is small compared to the $CO_2$-induced changes in intensity. It would be preferable to avoid this assumption and simulate tropical cyclone genesis and intensification explicitly within the global models themselves as part of the transient climate change experiments. Unfortunately, the enormous computation demands of constructing a global climate model capable of resolving tropical cyclones of realistic intensity and spatial scale remains beyond the capability of present-day climate modeling centers, which is why we use the nested downscaling approach for our study.

## 3. Global model climate change scenarios

The large-scale boundary conditions (i.e., SST, atmospheric temperature, and water vapor) for the hurricane model experiments are derived from climatologies from nine different global coupled ocean–atmosphere climate models participating in the CMIP2+ intercomparison project (Table 1). Background information on all of the models except version 2.3 of the Meteorological Research Institute Coupled General Circulation Model (MRI CGCM 2.3) is available in Table 8.1 of McAvaney et al. (2001). Information on the MRI CGCM2 is contained in the above table as well as in Yukimoto and Noda (2002). Control and +1% $yr^{-1}$ compounded $CO_2$-increase experiments were available for each model. The +1% $yr^{-1}$ compounded $CO_2$-increase scenario represents an idealized greenhouse gas-forcing scenario, rather than a forecast of future radiative forcing. Other radiative forcing agents besides greenhouse gases may have important effects on global climate, although quantification of their past and possible future forcing remains even more uncertain than for greenhouse gases. For each CMIP2+ model, the SST, air temperature, atmospheric humidity, and surface pressure fields were obtained. Area-averaged time series were computed for July–November over the following three tropical cyclone basins and seasons: (i) northwest (NW) Pacific: 8°–26°N, 124°–161°E; (ii) NW Atlantic: 10°–26°N, 49°–79°W; and (iii) northeast (NE) Pacific: 10°–19°N, 101°–131°W. Although we did not perform hurricane model experiments for the remaining three tropical storm basins [north Indian, south Indian, and southwest (SW) Pacific], preliminary statistics for those basins indicate that the behavior of the three basins that we analyzed in detail is representative of the other basins as well.

For the control or ''present-day'' conditions, an 80-yr mean seasonal climatology from the control runs was used. Linear trends were computed from the seasonal +1% run time series in order to derive a high-$CO_2$ climate. The high-$CO_2$ climate was defined as the sum of the control run mean plus an 80-yr net linear trend component (taken as the +1% experiment trend minus the control run trend) and thus represents ''warm climate'' conditions resulting from an 80-yr buildup of $CO_2$. The 80-yr trend component from the control run was included to account for the effect of possible drift in the control runs. One of the models (ECHAM–OPYC) showed a pronounced ''cold start,'' or delay in the onset of a quasi-linear trend, in the +1% $yr^{-1}$ $CO_2$ experiment. To reduce the bias from this cold start, the linear trends for this model were computed over years 31–80 of the +1% run and then adjusted by the factor 8/5 to obtain the 80-yr trend for our experiments. For the Third Hadley Centre Coupled Ocean–Atmosphere General Circulation Model (HadCM3), the linear trends from the +1% run were computed over years 22–80 and then adjusted to an 80-yr trend due to a missing data problem earlier in the record. The +1% $yr^{-1}$ compounded increase in $CO_2$ results in levels higher by a factor of 2.22 by year 80 of the CMIP2+ experiments for all of the models except the GFDL climate model. In the GFDL +1% experiment, the $CO_2$ level reaches twice its initial value after 70 yr, as in the other models, but is then held fixed at $2 \times CO_2$ for years 71–80. This leads to a slight negative bias in the 80-yr warming trend for the GFDL model relative to the other models.

Figure 2 shows the SST changes (80-yr net trends) for the CMIP2+ models for each of the three tropical storm basins. All models show a substantial $CO_2$-induced tropical SST increase, varying from +0.8° to +2.4°C. Figure 2 indicates that there is considerable uncertainty in regional warming rates for the tropical storm basins due to differing climate sensitivity, ocean heat uptake, and other regional-scale processes in the models. Although not assessed here, considerable uncertainty in future warming rates also arises due to certainties in future anthropogenic emission scenarios and radiative forcing. Note that although the $CO_2$ levels have reached about 2.2 times the control run values by year 80 (except for the GFDL model, as noted above), the coupled CMIP2+ models have not fully equilibrated to the $CO_2$ increase—a process that can take several thousand simulation years (Stouffer 2004). For example, in one published transient coupled model experiment (Manabe et al. 1991, see their Fig. 12c) only about 3/4 of the equilibrium surface temperature response to a doubling of $CO_2$ is attained in the tropical storm basins by year 70 (the time of $CO_2$ doubling) in a +1% $yr^{-1}$ $CO_2$ increase experiment. This ''thermal inertia'' of the

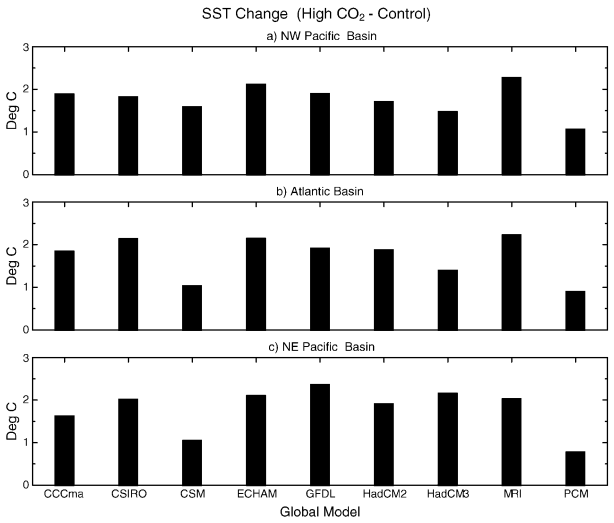


FIG. 2. SST change (high $CO_2$ − control) in °C for each CMIP2+ climate model (bottom axis label) for the (a) NW Pacific, (b) Atlantic, and (c) NE Pacific basins. This represents the warming that occurs in the tropical storm basins and tropical storm seasons over an 80-yr period during which atmospheric $CO_2$ concentrations increase at 1% $yr^{-1}$ compounded in the model. See text for further details.

simulated climate system is generally even greater in higher-latitude regions than in the Tropics.

A characteristic feature of the $CO_2$-induced warming among the CMIP2+ models is an enhanced warming of the upper tropical troposphere relative to the surface. This is illustrated in Fig. 3, showing the tropical mean temperature change profile of each model, normalized by dividing by the warming at the lowest atmospheric level. The ECHAM–OPYC model shows the greatest upper-tropospheric warming enhancement, whereas the Commonwealth Scientific and Industrial Research Organisation (CSIRO) and GFDL models show less upper-tropospheric warming enhancement than the other models. The enhanced upper-tropospheric warming is likely a result of the tendency of models to adjust their temperature lapse rates in the Tropics toward a moist adiabatic profile. Since moist adiabats in warmer atmospheres have a smaller temperature decrease with height than those in cooler atmospheres, a decrease in the dry lapse rate occurs.

While the CMIP2+ models are in fairly good agreement with regard to an upper-tropospheric enhancement of the $CO_2$-induced surface warming, it is worth noting that observed tropospheric temperature trends over the late twentieth century do not show as much upper-tropospheric enhancement of warming as model simula-

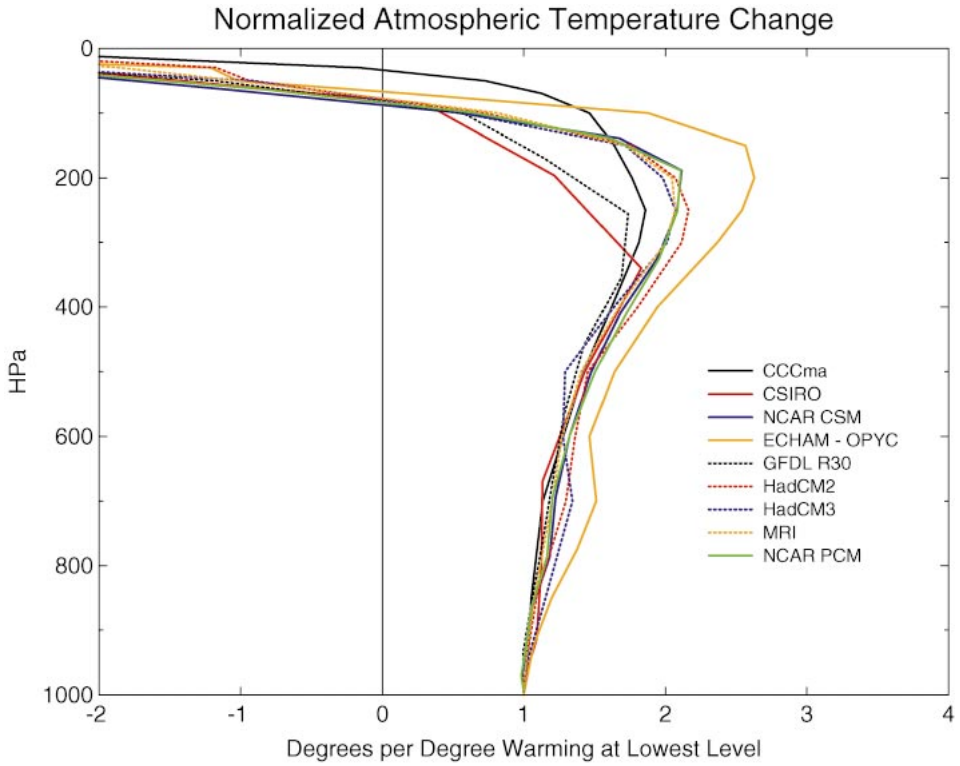


FIG. 3. Normalized atmospheric temperature change (high $CO_2$ − control) vertical profiles, zonally averaged over all latitudes from 20°N to 20°S. The difference is based on years 61–80 of the high $CO_2$ run minus years 61–80 of the control run for each CMIP2+ model (legend). The difference at each model level is normalized by dividing by the difference at the lowest level for that model.

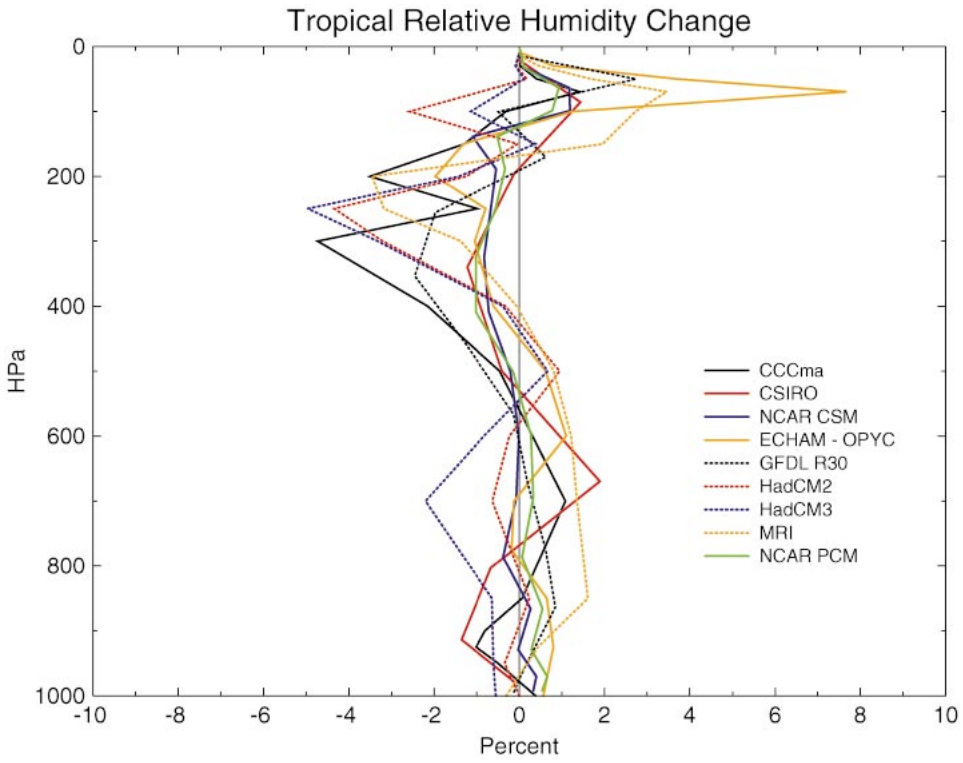


FIG. 4. As in Fig. 3, but for relative humidity (in %). No normalization of the differences was done.

tions, even when models include a more realistic historical forcing (e.g., Santer et al. 1996; Tett et al. 1996; Hansen et al. 2002). Whether this discrepancy is due to model error, incorrect or incomplete radiative forcing, or observational data problems remains unresolved. The modeling studies show that the simulated vertical profile of temperature change in the Tropics can be sensitive to the type of radiative forcing applied. This implies that a more realistic radiative forcing scenario, with changes in several atmospheric trace constituents and surface properties, could produce a somewhat different profile of temperature change relative to the surface than that shown in our Fig. 3 (based on a $CO_2$ increase only). Nonetheless, more complete future radiative forcing scenarios developed for recent climate change assessments show $CO_2$ making up an increasingly greater fraction of the total radiative forcing over the coming century (Houghton et al. 2001).

The tropical mean relative humidity change profiles for the CMIP2+ models are shown in Fig. 4. In the lower troposphere, the models simulate relatively small changes—generally in the range of $\pm 2\%$. In the upper troposphere, from about 400 to 200 mb, there is a systematic tendency among the models for a reduction in relative humidity, although the change is again relatively small, ranging from about $-1\%$ to $-5\%$, based on the years 61–80 of the $+1\%$ runs. The small change in lower-tropospheric relative humidity, together with the pronounced atmospheric warming, implies a substantial increase in tropospheric water vapor content under high $CO_2$ conditions, a point we will return to later in this report.

In summary, the CMIP2+ models' response to a $+1\%\ yr^{-1}$ increase in $CO_2$ includes a substantial warming of tropical storm basin SSTs, enhanced upper-tropospheric warming relative to the surface warming, and little change in lower-tropospheric relative humidity. Previous modeling studies (Knutson and Tuleya 1999; Shen et al. 2000) have indicated the relative roles of SST and upper-tropospheric warming in affecting hurricane intensities. The impact of the $CO_2$-induced changes in environmental conditions from the CMIP2+ models on simulated hurricane intensities is quantitatively explored in the remainder of this paper.

## 4. Simulation results

### *a. Storm intensity and precipitation changes*

A series of 5-day idealized simulations of the hurricane model were performed using the methodology described in section 2. They tested different combinations of GCM environmental conditions (nine different climate models), climate scenario (control or high $CO_2$), tropical storm basin (three different basins), cumulus convection scheme in the hurricane model (four different versions), and small random perturbations to initial conditions (ensemble size of 6 for each combination of

the above factors). Thus a total of 1296 experiments ($9 \times 2 \times 3 \times 4 \times 6$) were performed and are analyzed in this section.

Time series of minimum central pressure from all of the sensitivity experiments for two of the nine CMIP2+ models (GFDL R30 and HadCM2) are shown in Fig. 5. These examples are representative of the features seen for the remaining seven climate models. There is a clear tendency for more intense hurricanes (lower central pressures) for the high-$CO_2$ conditions (solid lines) than for the control run or present-day conditions (dotted lines). For the analysis in the remainder of the study, we use the intensity averaged over hours 97–120 of the experiments as an approximation for the ''equilibrium intensity'' of the storm. Although this approximation is clearly not met for many of the storms in Fig. 5 (e.g., GFDL/Emanuel convection for the Atlantic and Pacific), it does appear that in most cases at least the difference between control and high-$CO_2$ cases has reached a quasi equilibrium by day 5 of the experiments. Notable exceptions are the HadCM2/Kurihara convection runs for the Atlantic and NW Pacific basins, where the differences between the control and high-$CO_2$ runs still appear to be increasing at the end of 5 days. In several of the experiments the storm intensifies very rapidly during the first day or so of the simulation, apparently ''overshooting'' its final intensity before decreasing in intensity during days 2–5. Another characteristic of the experiments illustrated by Fig. 5 is the varying degree of scatter between individual members of the six-member ensembles. Some of the sensitivity cases show a very tight grouping of the six ensemble members, whereas others (e.g., GFDL GCM/Kurihara convection scheme) show much more scatter between the ensemble members. The latter illustrate why an ensemble approach is highly desirable even for this very idealized experimental design.

Figure 6 presents an overall summary of the intensity simulation results for all 1296 experiments in the study. The dark (light) curve shows the day-5 intensity distribution for the high-$CO_2$ (control) cases. The mean of the high-$CO_2$ cases is 10.4 mb lower (i.e., more intense) than the mean of the control cases. The pressure fall (environmental surface pressure minus central minimum pressure) is 13.7% greater on average for the high-$CO_2$ simulations. Although not evident in Fig. 6, which combines results from all the convection scheme sensitivity tests together, similar pressure fall increases are simulated for each of the individual convection schemes (see Table 2).

The bar along the top of Fig. 6 depicts the central pressure ranges for categories 3–5 of the Saffir–Simpson hurricane intensity scale. The shift toward higher intensities for the high-$CO_2$ cases appears to be equivalent to about half a category on this scale. Substantially more storms reach category 5 for the high-$CO_2$ conditions than for the control conditions. Although our experiment by design cannot address the issue of future changes in overall tropical storm frequency, our results suggest an increase in the relative risk of occurrence of category-5 hurricanes under high-$CO_2$ conditions.

Intensity simulation results in terms of maximum surface wind speeds are shown in Fig. 7. Separate pairs of histograms are shown for each version of convection parameterization tested with the hurricane model. The control condition storms are least intense for the Emanuel convection runs ($\sim$50 m $s^{-1}$), and of similar intensity for the other schemes (61–62 m $s^{-1}$). All of the schemes show a clear shift in the histogram toward more intense storms under high-$CO_2$ conditions. The percentage increases are quite similar for the different schemes, ranging from 5.0% to 7.0%. Combining the results for the different schemes, the overall increase of intensity in terms of maximum surface wind speeds amounts to 5.8% for the high-$CO_2$ conditions.

Precipitation simulation results for the experiments are summarized in Fig. 8. Separate pairs of histograms are shown for each convection scheme because the different convection treatments yield quite different control run precipitation rates. The primary statistic used here to assess precipitation is the instantaneous precipitation rate averaged within a 100-km radius of the storm center (central pressure minimum) at hour 120. The mean of the distributions for the control runs varies from 56 cm $day^{-1}$ for the Emanuel convection scheme to 99 cm $day^{-1}$ for the Pan scheme. The simulations for all of the convection schemes show a marked increase in precipitation rate for the high-$CO_2$ cases compared to the controls. The percentage increase in the mean varies from 12%–13% for the Kurihara and resolved convection cases to 22%–26% for the Emanuel and Pan convection cases. These are substantially higher percentage changes than simulated for the maximum surface wind speeds ($\sim$6%). In all cases the increase for the high-$CO_2$ distributions is highly statistically significant. Specifically, for each of the four sets of distributions shown in Fig. 8, the null hypothesis that the control and high-$CO_2$ samples come from the same population can be rejected ($P < 0.001$) in favor of the predicted hypothesis that the population from which the high-$CO_2$ sample is drawn has stochastically larger values than that of the control sample. The test used for this assessment was the Kolmogorov–Smirnov one-sided, two-sample distribution test (e.g., Siegel and Castellan 1988, 144–151).

Other measures of storm precipitation have also been analyzed. Results for two such alternative measures are summarized in Table 2: the maximum precipitation rate anywhere in the domain and the area-averaged precipitation rate over the entire $5° \times 5°$ innermost mesh of the hurricane model. All of the precipitation measures show an increase in precipitation rate for the high-$CO_2$ cases. The percent change for the domain maximum precipitation rate typically shows the largest percentage increase of the three measures, varying from 17% for resolved convection to 33% for Kurihara convection. The percent changes are much smaller for the $5° \times 5°$

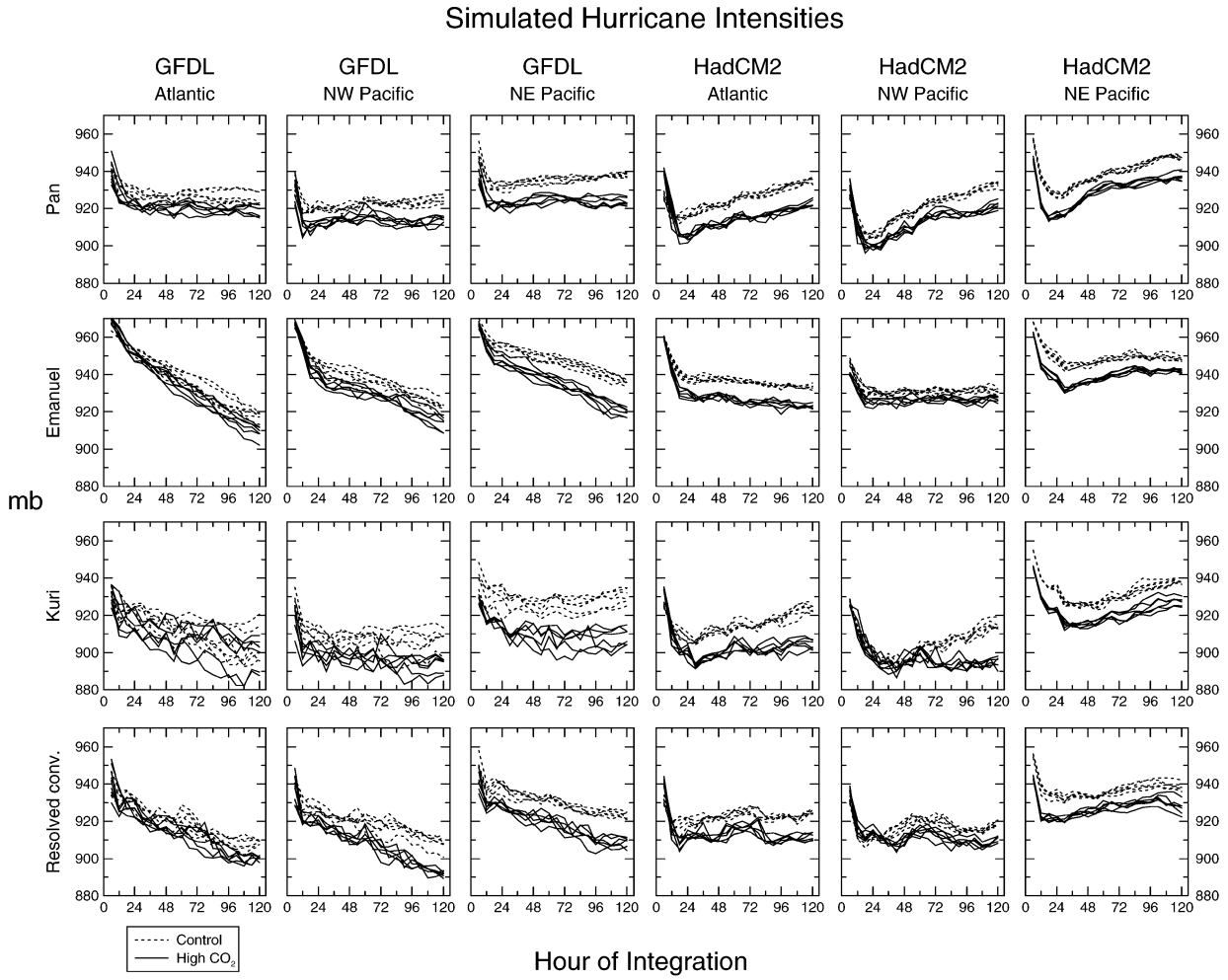


FIG. 5. Time series of minimum central pressures (mb) from 5-day idealized hurricane model experiments using large-scale environmental conditions from the GFDL (columns 1–3) or HadCM2 (columns 4–6) climate models. The dotted and solid lines show the six ensemble members for the control and high-$CO_2$ conditions, respectively (see legend). The convection schemes used in the hurricane model include Pan (top row); Emanuel (row 2); Kurihara (row 3); and resolved inner-grid convection with Emanuel convection in the outer two grids (bottom row).

domain-averaged precipitation, ranging from 2.7% (Kurihara convection) to 8.8% (Pan convection). In comparison, the low-level environmental specific humidity is 13% greater on average in the high-$CO_2$ environments than in the controls (Table 2). These results suggest that precipitation rates near the core region of the hurricane increase by a greater percentage than the low-level moisture content; thus, the enhanced precipitation in the high-$CO_2$ storms may result from enhanced moisture convergence due to both enhanced low-level moisture content and enhanced convergence associated with the more intense storm circulation.

In Fig. 9, the aggregate central pressure results shown in Fig. 6 are disaggregated by convection scheme and basin. For this figure, each bar represents the percent change in the ensemble mean pressure fall for a given basin, the CMIP2+ climate model, and the hurricane model convection scheme. The change in pressure fall is positive (greater intensity for high-$CO_2$ cases) for every combination of basin, convection scheme, and CMIP2+ climate model, except for one of the Atlantic cases for Emanuel convection, which was very slightly negative. Another Atlantic basin case using resolved convection was only slightly positive ($<+1\%$). On the high end, the percentage changes were more than +30% in two of the combinations. Overall, the percent change in pressure fall is rather similar across the different convection schemes, varying from about 13% to 15% (Table 2).

Similar results to those shown in Fig. 9 are obtained for maximum surface wind speeds (not shown), except that the percentage changes are generally smaller for wind speed (aggregate change of +5.8%). A plot similar to Fig. 9, but for precipitation rate (not shown), indicates a much stronger dependence of the percent changes on the convection scheme used, as can be anticipated from

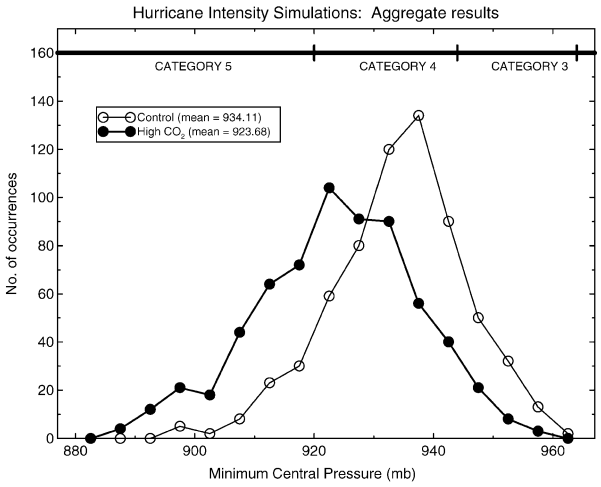


FIG. 6. Frequency histograms showing hurricane intensity results (mb) aggregated across all 1296 experiments performed for the study. The histograms are formed from the min central pressures, averaged over the final 24 h from each 5-day experiment. The light (dark) line with open (solid) circles shows results for the control (high $CO_2$) cases (see legend). The central pressures for experiments using data from each of nine different CMIP2+ climate models and three tropical storm basins, and using four different convective parameterization treatments and six ensemble members differing only slightly in their initial conditions, all are combined to form a single histogram for either the control or high $CO_2$ cases.

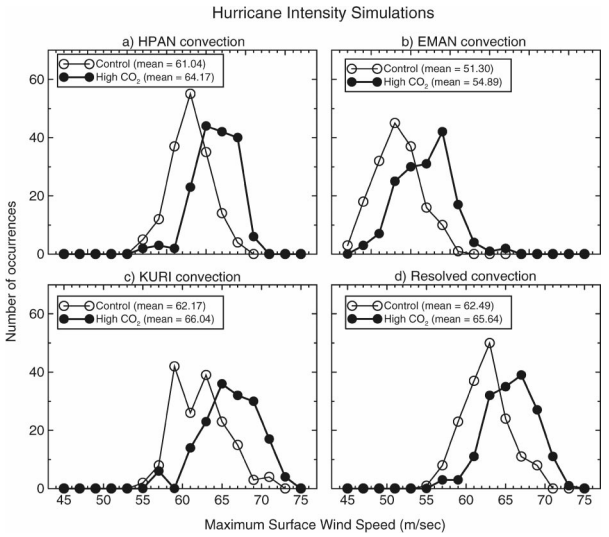


FIG. 7. As in Fig. 6, except for max surface wind speed (m $s^{-1}$). For this figure, separate pairs of histograms were constructed for each convection scheme treatment: (a) Pan convection, (b) Emanuel convection, (c) Kurihara convection, and (d) resolved inner-grid convection with Emanuel convection used in the outer two grids.

Fig. 8 and Table 2. Also, in the case of precipitation, 2 of 108 basin/CMIP2+ model combinations gave a slightly negative change, whereas on the high side, the positive changes ranged up to 50% or more for a few combinations.

Figure 10 shows the percent change in pressure fall, similar to Fig. 9, but groups the results for each basin by individual CMIP2+ climate model rather than by convection scheme. Figure 10 shows that there is a tendency for smaller percentage changes in central pressure for the two National Center for Atmospheric Research (NCAR) models [Climate System Model (CSM) and Parallel Climate Model (PCM)] than for the other CMIP2+ models, although a fairly large positive change is simulated for the CSM in the case of the NW Pacific basin, and a relatively small percent change is simulated for the GFDL CMIP2+ model for the Atlantic basin. The largest percent increases are simulated for the MRI model, while the HadCM3, GFDL, and CSIRO models

TABLE 2. Summary of simulation results for various storm intensity and precipitation measures from the idealized hurricane experiments performed for the present study. The PI, CAPE, and boundary layer specific humidity values are for the large-scale environmental conditions that were used to derive the initial conditions and boundary conditions for the hurricane model simulations. The columns show hurricane model results grouped by convection scheme (see text). The columns labeled ''% Change'' show the percent change in the metric between the control and high-$CO_2$ conditions. For pressure measures the % Change refers to percent change in pressure fall (environmental surface pressure minus central min pressure).

| | All convection schemes | | HPAN | | EMAN | | KURI | | Resolved | |
|---|---|---|---|---|---|---|---|---|---|---|
| | Control | % Change | Control | % Change | Control | % Change | Control | % Change | Control | % Change |
| Max surface wind speed (m $s^{-1}$) | 59.2 | 5.8% | 61.0 | 5.1% | 51.3 | 7.0% | 62.2 | 6.2% | 62.5 | 5.0% |
| Min central pressure (mb) | 934.11 | 13.7% | 938.15 | 13.4% | 942.75 | 13.3% | 926.48 | 15.4% | 929.07 | 12.7% |
| PI (Emanuel, mb) | 908.83 | 7.5% | | | | | | | | |
| PI (Holland; mb) | 927.59 | 15.9% | | | | | | | | |
| CAPE (J $kg^{-1}$) | 1924.8 | 20.6% | | | | | | | | |
| Precipitation (100-km radius; cm $day^{-1}$) | 80.2 | 18.3% | 99.4 | 26.2% | 56.1 | 22.2% | 76.6 | 12.9% | 88.7 | 11.6% |
| Precipitation (max in domain; cm $day^{-1}$) | 706.2 | 23.9% | 697.0 | 27.6% | 581.7 | 19.4% | 652.9 | 32.9% | 893.4 | 17.3% |
| Precipitation (inner-nest avg; cm $day^{-1}$) | 1.62 | 6.7% | 1.74 | 8.8% | 1.27 | 8.7% | 2.18 | 2.7% | 1.28 | 8.6% |
| Boundary layer specific humidity (g $kg^{-1}$) | 17.07 | 12.7% | | | | | | | | |

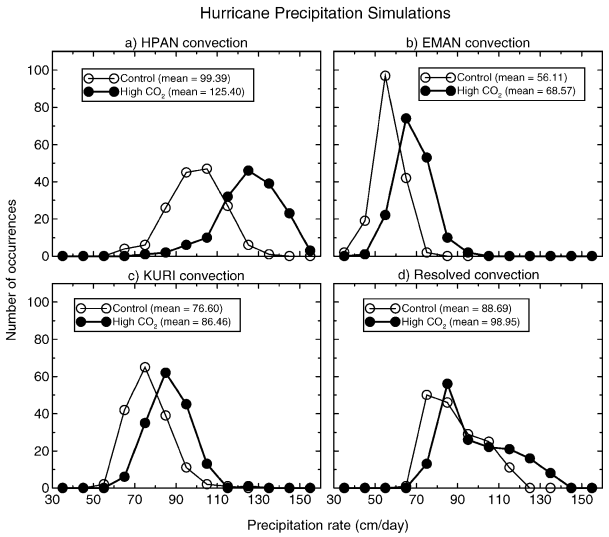


FIG. 8. As in Fig. 7, except for the instantaneous precipitation rate (cm day$^{-1}$) at simulation hour 120, spatially averaged over all grid points within a 100-km radius of the central pressure min for each storm.

all have cases of quite substantial (more than +20%) increases for some basins.

Although not shown here, the results in Fig. 10 can be normalized by the sea surface temperature changes for each CMIP2+ model (Fig. 2), in which case they exhibit less variation than in Fig. 10, as might be expected. As noted in the discussion of Fig. 2, the NCAR models (CSM and PCM) had smaller increases in tropical storm basin SSTs than the other CMIP2+ models. This appears to be a major reason why they produce smaller storm intensification than the other CMIP2+ models in our simulations.

For the main simulations presented in this paper, the $CO_2$ content in the hurricane model remains unchanged from its control run value, even for the high-$CO_2$ cases. The effect of higher $CO_2$ in the climate models is assumed to be adequately incorporated into the hurricane model simulations indirectly through changes in the (specified) SSTs and atmospheric boundary and initial conditions from the global models. To justify this assumption, an ensemble set ($n = 6$) of auxiliary runs was performed for one case in which the $CO_2$ concentration was increased by a factor of 2.2, leaving the SST and other boundary/initial conditions at their control run values. Changing the $CO_2$ level alone results in a statistically insignificant 1-mb decrease in central pressure, compared to a statistically significant 10-mb decrease when SSTs and atmospheric boundary and initial conditions (but not $CO_2$) are modified. Thus the effect of SST and atmospheric boundary and initial condition changes overwhelms any minor direct effect of $CO_2$ changes in these 5-day regional model experiments.

### *b. Relationships between simulations and environmental variables*

In this section, we explore relationships between the simulated intensities (or precipitation) and some environmental measures that can be derived directly from the CMIP2+ model fields. Scatterplots of simulated hurricane intensity versus SST are shown in Fig. 11. Results for the different hurricane model convection schemes are plotted in four separate scatterplots. The correlation between SST and simulated intensity is fairly high in absolute value, ranging from −0.64 for the Emanuel scheme (control) to −0.84 for the Kurihara high-$CO_2$ cases. A clear relationship exists in the model: higher SSTs correlate with higher simulated intensities. The high-$CO_2$ linear regression lines are not simple extensions of the control regression lines but are shifted to the right, indicating that for a given SST value, the simulated intensity is higher for the control runs than for the high-$CO_2$ runs. The magnitude of the shift is on the order of 5–10 mb. This feature is likely an effect of the enhanced upper-tropospheric warming in the CMIP2+ model high-$CO_2$ environments (Fig. 3). As shown by Shen et al. (2000), enhanced upper-tropospheric warming relative to the surface warming reduces the intensity of simulated storms. In other words, the SST increases and enhanced upper-tropospheric warming in the high-$CO_2$ environments have opposing effects on simulated intensities, with the SST effect evidently dominating, since there is a net increase in storm intensities for the high-$CO_2$ storms.

A clear statistical relationship also exists between convective available potential energy (CAPE) and intensity, with greater simulated intensities for environments with greater CAPE (Table 3). The absolute correlation coefficients are slightly smaller than for SST, ranging from −0.65 to −0.72. As shown in Table 2, the aggregate percent change in CAPE is 21%, which is substantially larger than the aggregate percent change in either pressure fall (14%) or surface wind speeds (5.8%). Enhanced CAPE for the high-$CO_2$ environments was found for 26 of 27 CMIP2+ model/basin combinations, despite the enhanced upper-tropospheric warming in the models. Enhanced CAPE is consistent with theories suggesting a relationship between higher CAPE and warmer climates (e.g., Renno and Ingersoll 1996).

Correlations between simulated intensities and tropical cyclone potential intensity (PI) measures are also presented in Table 3. These PI estimates are based on the methods of Emanuel (1986, 1988, 1995) and Holland (1997). The Emanuel method as applied here assumes pseudoadiabatic ascent and neglects dissipative heating. The hurricane model–simulated intensities for all convection treatments are positively correlated with both of the PI estimates, although the correlations (ranging from 0.3 to 0.76) are typically smaller than the absolute correlations were between simulated intensity and either SST or CAPE, as shown in Table 3.

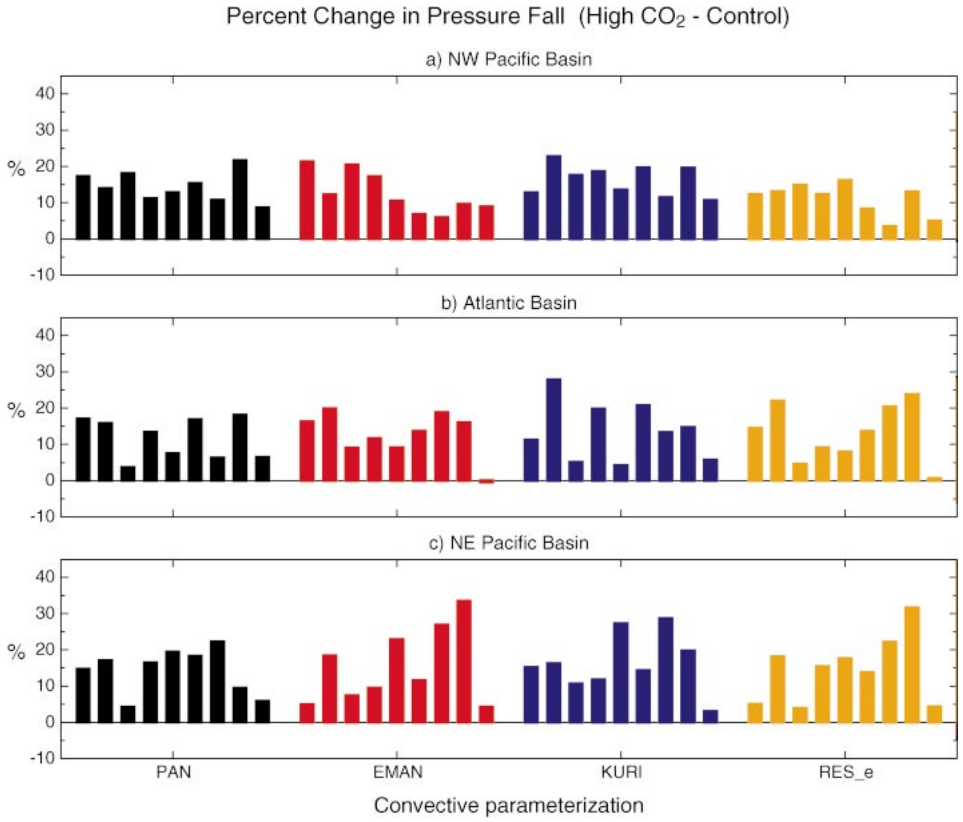


FIG. 9. The percent change in pressure fall (high $CO_2$ vs control) for the idealized hurricane simulations. A positive change indicates stronger storms (i.e., a greater pressure fall from the large-scale environmental surface pressure). The results are shown for the (a) NW Pacific, (b) Atlantic, and (c) NE Pacific basins, respectively, and are grouped according to the convective parameterization method used in the hurricane model: PAN (black bars), EMAN (red), KURI (blue), and RES_e (gold; refers to resolved inner-grid convection with the Emanuel scheme used in the outer two model domains). Each bar represents the ensemble mean result for a single CMIP2+ model (not separately identified) and is calculated by comparing the ensemble mean ($n = 6$) pressure fall for the high-$CO_2$ cases with the ensemble mean ($n = 6$) for the control cases.

Figures 12 and 13 show the relationship between simulated intensity differences (high $CO_2$ − control) and differences in PI (high $CO_2$ − control) in terms of percent change in pressure falls. Separate scatterplots are shown for each hurricane model convection treatment. The same PI values are used in Figs. 12a–d and 13a–d, as they depend only on the imposed environmental state and are independent of the hurricane model. There is a substantial positive correlation between the simulated intensity changes and the changes predicted by the PI theories, ranging from about 0.4 to 0.7. The results clearly indicate higher PI under high-$CO_2$ conditions. The aggregate percent increase is 7.5% for the Emanuel method (Fig. 12; Table 2) and 16% for the Holland method (Fig. 13; Table 2) as compared with 14% for the simulations. In terms of central pressure, the mean intensification (central pressure decrease) averaged across all three basins and nine CMIP2+ models (high-$CO_2$ cases versus control) is 8 mb for the Emanuel method and 13 mb for the Holland method. Thus, while there are substantial differences between the PI theories and their assumptions (Camp and Montgomery 2001), both theories predict a similar aggregate intensification in the high-$CO_2$ environments to that simulated with the hurricane model (10 mb). Previous studies (Emanuel 1987; Tonkin et al. 1997) have found substantial increases in PI for $2 \times CO_2$ equilibrium climate change conditions based on earlier global climate models.

Figure 14 shows scatterplots of the simulated precipitation rates (within 100 km of the storm center) versus the SST. The correlations are quite high for the three convective parameterizations (0.69–0.89) compared to the resolved convection experiments (0.24 for the high $CO_2$ and negligible for the control). For the three parameterized convection cases (Figs. 14a–c), the high-$CO_2$ regression lines are nearly coincident with the control regression line, implying that the high-$CO_2$ precipitation results could have been anticipated by extrapolating the control run SST versus the precipitation regression relationship using the higher SSTs from the high-$CO_2$ environments. Although not discussed here, some additional regression calculations between inten-

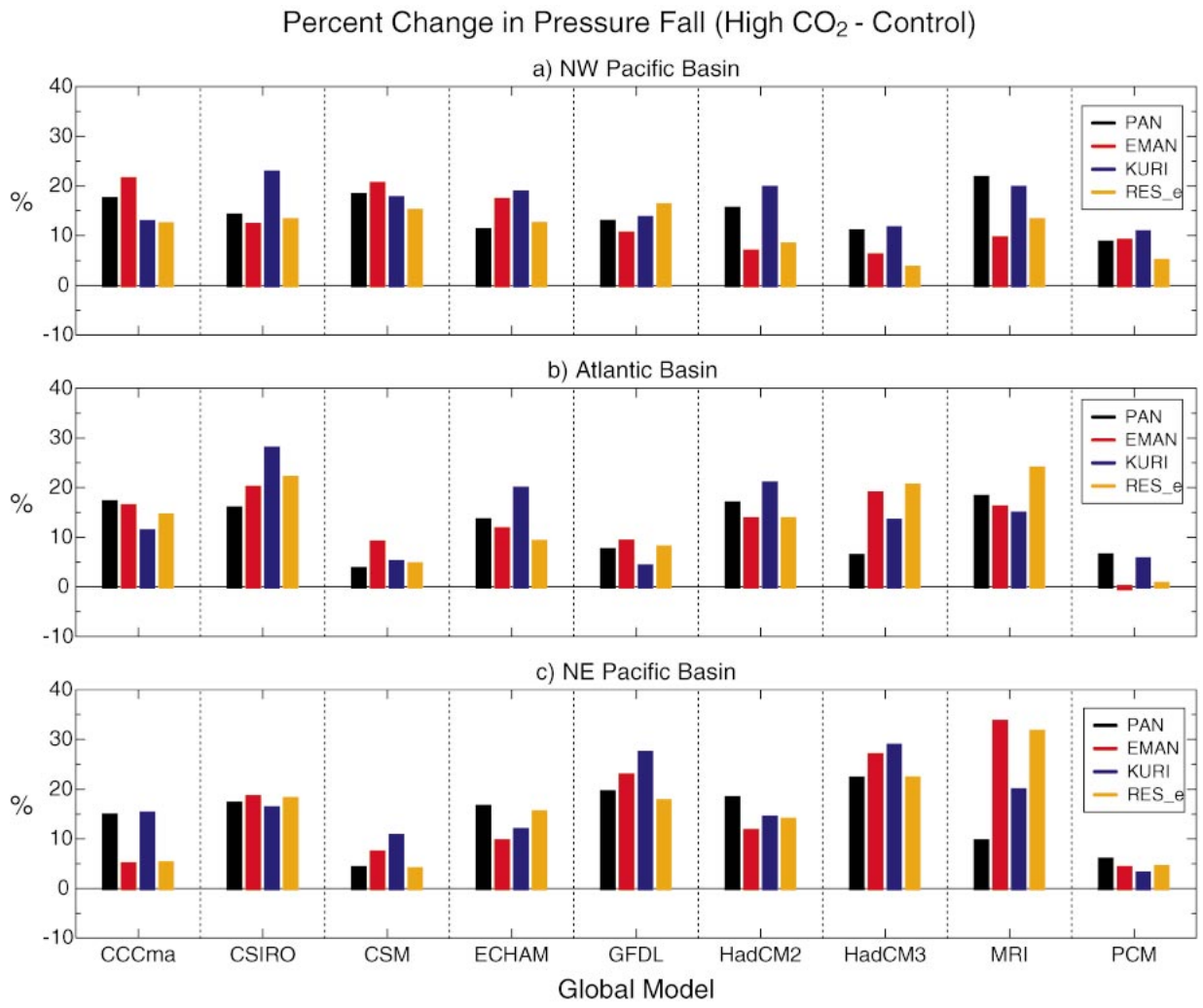


FIG. 10. As in Fig. 9, except that the results are grouped according the CMIP2+ model from which the large-scale thermodynamic environmental conditions have been derived (see bottom axis labeling). The convection scheme used in the hurricane model (see legend and Fig. 9 caption) can be identified by the color of the bars.

sity or precipitation and various environmental measures are included in Table 3.

## 5. On the role of vertical wind shear

As noted earlier, potential dynamical influences on intensity such as wind shear are not included in the experiments for this study. Both the theoretical PI methods of Emanuel and Holland and our idealized hurricane simulation studies (e.g., Knutson et al. 2001) attempt to quantify the influence of the thermodynamic environment (SST, atmospheric temperature, and moisture) on tropical cyclone intensity and do not explicitly address the question of possible large-scale dynamical influences. However, dynamical influences are believed to play an important role in determining the frequency of occurrence of tropical cyclones and their intensification (e.g., Gray 1968; McBride and Zehr 1981; Kurihara and Tuleya 1981; DeMaria and Kaplan 1994; Vitart et al. 1999).

Such dynamical influences may provide an explanation for the statistical observation (Emanuel 2000) that tropical cyclones in the Atlantic and NW Pacific basins, once reaching hurricane strength, have a roughly equal probability of reaching any intensity from minimal hurricane intensity up to, but not exceeding, their PI. Studies by Emanuel (2000) and Tonkin et al. (2000) support the contention that, dynamical influences notwithstanding, the potential or upper-limit intensity of tropical cyclones can be reasonably estimated based on knowledge of the large-scale thermodynamic environment alone. Emanuel (1999) furthermore used a highly simplified numerical model to demonstrate that for many recent cases, the evolution of hurricane intensity can be simulated from knowledge of the storm's initial intensity, the large-scale thermodynamic state of the at-

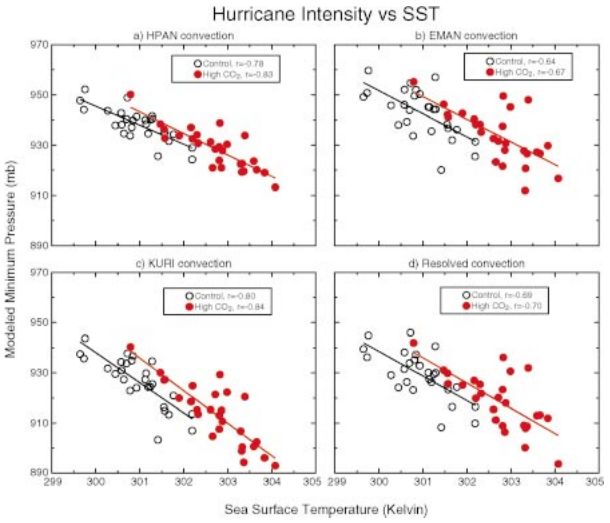


FIG. 11. Scatterplots showing the relation between simulated hurricane intensity in terms of min central pressure (mb) and the specified SST (K) for the experiment. Results are shown separately for hurricane model simulations using the same convection schemes as in Fig. 7. The open and solid red circles show results for the control and high-$CO_2$ cases, respectively. Each circle represents an ensemble mean ($n = 6$) result for a particular basin (NW Pacific, Atlantic, or NE Pacific) and a CMIP2+ model large-scale environment. Thus there are $3 \times 9 = 27$ control and 27 high-$CO_2$ circles on each scatterplot. The lines show the linear regression through each set of 27 data points; correlation coefficients are reported in the legends.

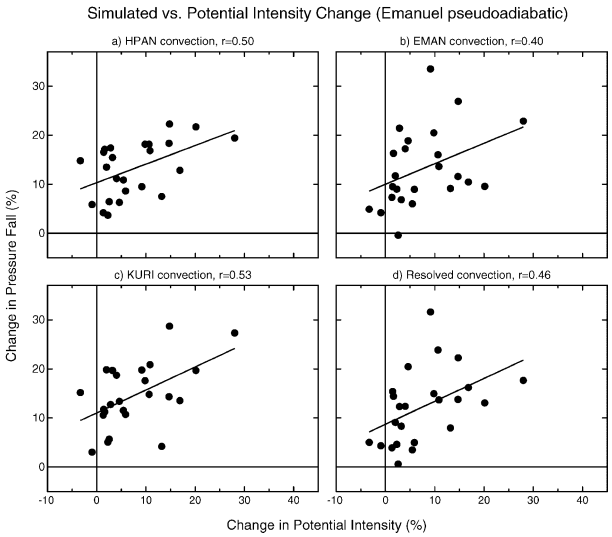


FIG. 12. As in Fig. 11, except that the simulated change in pressure fall (high $CO_2$ vs control) is compared with the change in pressure fall for the large-scale environmental conditions according to the PI theory of Emanuel. See text for further details. A positive change indicates a greater pressure fall (stronger storm) for the high-$CO_2$ cases. For the CSIRO model, extremely large percent changes in pressure fall were obtained for each of the basins (+150% to +200%) using the Emanuel method. We considered these results implausible and speculate that they were artifacts of the very coarse vertical resolution of the CSIRO model (only 9 vertical levels). Therefore, these data were excluded from this figure and our other analyses of Emanuel PI.

TABLE 3. Correlations between simulated hurricane intensity or precipitation and various measures of the thermodynamic environment used to derive the boundary conditions and initial conditions for the hurricane simulations. The intensity metric is the min central pressure averaged over day 5. The precipitation metric is the instantaneous precipitation rate at hour 120 averaged within 100 km of the storm center. Delta refers to the change from control to high-$CO_2$ conditions. Delta intensity, delta PI and delta CAPE correlations are computed using percent changes in pressure fall and percent changes in CAPE. See captions for Figs. 11–14 for further details on the samples.

| | HPAN | | EMAN | | KURI | | Resolved | |
|---|---|---|---|---|---|---|---|---|
| | Control | High $CO_2$ | Control | High $CO_2$ | Control | High $CO_2$ | Control | High $CO_2$ |
| Intensity vs | | | | | | | | |
| SST | −0.78 | −0.83 | −0.64 | −0.67 | −0.80 | −0.84 | −0.69 | −0.70 |
| CAPE | −0.66 | −0.66 | −0.70 | −0.71 | −0.67 | −0.65 | −0.72 | −0.70 |
| PI (Emanuel*) | 0.36 | 0.53 | 0.33 | 0.43 | 0.41 | 0.61 | 0.33 | 0.44 |
| PI (Holland) | 0.48 | 0.76 | 0.31 | 0.51 | 0.38 | 0.67 | 0.35 | 0.58 |
| Precipitaton | | | | | | | | |
| SST | 0.83 | 0.89 | 0.76 | 0.71 | 0.69 | 0.72 | 0.07 | 0.24 |
| Specific humidity | 0.52 | 0.63 | 0.64 | 0.58 | 0.44 | 0.48 | 0.33 | 0.34 |
| CAPE | 0.34 | 0.53 | 0.40 | 0.31 | 0.60 | 0.62 | 0.31 | 0.33 |
| Delta intensity vs | | | | | | | | |
| Delta SST | 0.77 | | 0.57 | | 0.70 | | 0.68 | |
| Delta CAPE | 0.75 | | 0.52 | | 0.58 | | 0.47 | |
| Delta PI (Emanuel*) | 0.50 | | 0.40 | | 0.53 | | 0.46 | |
| Delta PI (Holland) | 0.69 | | 0.38 | | 0.59 | | 0.37 | |
| Delta precipitation | | | | | | | | |
| Delta SST | 0.57 | | 0.55 | | 0.59 | | 0.08 | |
| Delta specific humidity | 0.55 | | 0.67 | | 0.50 | | 0.11 | |
| Delta CAPE | 0.44 | | 0.35 | | 0.39 | | −0.09 | |

* Assumes pseudoadiabatic ascent and neglects dissipative heating.

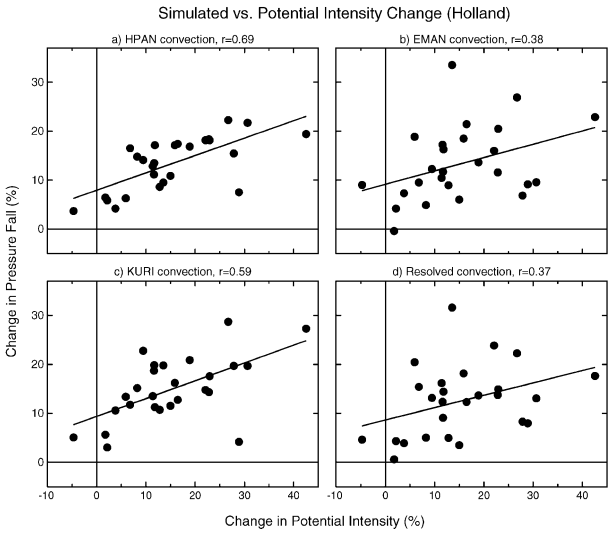


FIG. 13. As in Fig. 12, except for the PI theory of Holland. For the CSIRO model, the Holland code failed to converge to a solution for the Atlantic basin control conditions. We speculate that this result was an artifact of the very coarse vertical resolution of the CSIRO model (only 9 vertical levels). Therefore, data for CSIRO/Atlantic basin were excluded from this figure and our other analyses of Holland PI.

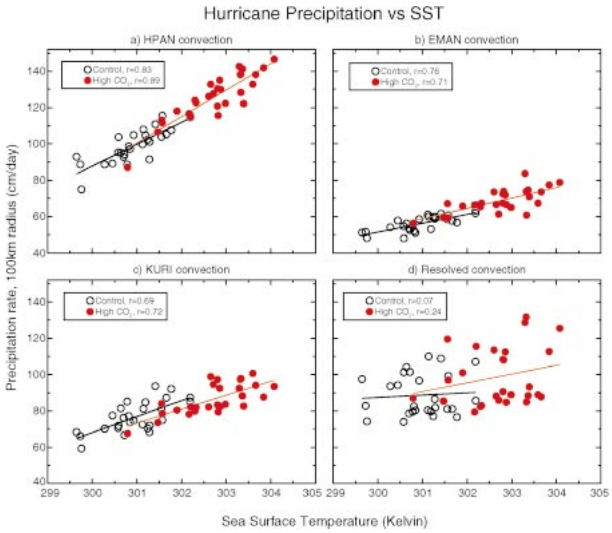


FIG. 14. As in Fig. 11, except for the instantaneous precipitation rate (cm day$^{-1}$) within 100 km of the storm center vs the SST (K).

mosphere, and heat exchange with the underlying ocean—without the need to model dynamical atmospheric influences. The relative importance of dynamical and thermodynamical influences on the intensity of strong hurricanes continues to be an area of active research.

Some attempts have been made to explicitly include dynamical influences in assessments of greenhouse gas–induced changes of intensity, using regional model ''case study'' approaches (Knutson and Tuleya 1999; Walsh and Ryan 2000). In these case studies, the tropical cyclone simulations incorporated more realistic synoptic environments including vertical wind shear. However, one can question how realistically the dynamical influences on the storms, such as vertical wind shear, are simulated—at least in the case of the GFDL hurricane model, for example, based on the performance of a recent operational version of that model in vertically sheared environments (M. DeMaria 2002, personal communication). In addition, we suspect that the time-mean vertical shear may be more relevant to the issue of tropical cyclone frequency (e.g., with unfavorably strong mean shear allowing fewer storms to develop over the course of a season) than to upper-limit intensities. For example, a very strong hurricane can occur in a season during which mean shear conditions are generally unfavorable, but a storm happens to occur during a temporary break in the unfavorable shear conditions due to normal synoptic weather variability. For these reasons, and the implication from Emanuel (2000) that one can obtain useful information on the relative distribution of hurricane intensities from knowledge of the potential intensity alone, we have chosen not to attempt to incorporate vertical shear in our idealized simulations for this study.

Although the influence of environmental wind shear is not included in our idealized simulations, it is nonetheless of interest to examine how the vertical shear changes in the CMIP2+ models. We focus on the tropical North Atlantic, where vertical wind shear appears to play a significant role in modulating major hurricane frequency (e.g., Goldenberg and Shapiro 1996; Goldenberg et al. 2001). Figure 15 compares the vertical profiles of the zonal wind for this basin—and its $CO_2$-induced change—among the different CMIP2+ models. The circles in Figs. 15a–i show the climatological zonal wind profile based on NCEP–NCAR reanalysis data for 1979–95 (Kalnay et al. 1996). In the control runs, all of the CMIP2+ models produce strong lower-tropospheric easterlies over the basin, although the vertical shear of the zonal wind is substantially too weak in a few of the models. In response to $CO_2$-induced warming, several of the models show some increase in vertical wind shear, with the most pronounced changes being in the ECHAM–OPYC model. Among the other models where some increase in vertical wind shear occurs (i.e., GFDL, HadCM2, HadCM3, and MRI), the changes are typically confined to the upper troposphere or lower stratosphere. Two of the models (CCCma and PCM) show decreases in vertical wind shear, and the remaining two (CSM and CSIRO) exhibit little change in mean shear.

The results shown in Fig. 15 for the Atlantic basin are fairly representative of the results for the other five basins (not shown). For example, in plots analogous to Fig. 15 for the other basins, there is a tendency for more mean vertical shear (in the high-$CO_2$ runs) typically for about half the models, with little change or a reduction

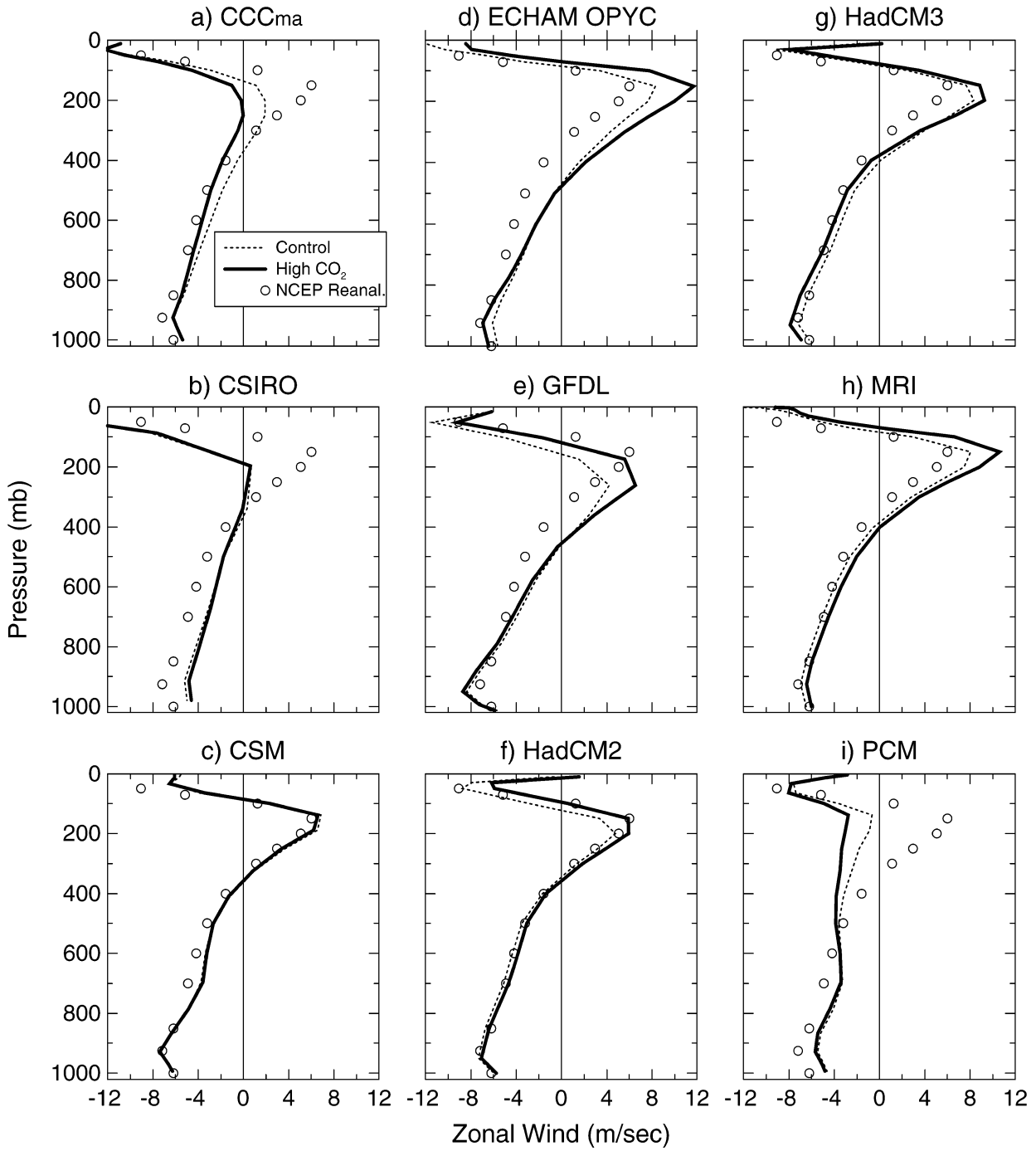


FIG. 15. Vertical profiles of the zonal wind (m $s^{-1}$) for the Atlantic tropical storm basin (averaged over Jul–Nov; 10°–26°N, 49°–79°W) obtained from each of the CMIP2+ models. The results for the control (years 61–80) and +1% $yr^{-1}$ $CO_2$ (years 61–80) experiments are denoted by the black dashed and solid lines, respectively. Open circles denote the observations according to the NCEP–NCAR reanalysis (1979–95).

in shear for the remaining models. In one of the basins (SW Pacific), substantially more shear is apparent in six of the nine models. In the North Indian Ocean, there is substantially more shear in only two of the nine models. With regard to comparisons of the control simulations and the NCEP–NCAR reanalysis, Fig. 15 is again fairly representative of results for all the basins, although the relative performance of the different models varies from basin to basin.

The vertical wind shear results suggest a tendency in

some models and in some basins toward a less conductive environment for tropical cyclogenesis in terms of vertical wind shear influence alone, although the results are quite model dependent, with typically about half the models indicating either the opposite tendency or little change. The vertical wind shear in the tropical storm basins thus appears to be an example of a regional climate feature for which the CMIP2+ models do not exhibit much agreement with regard to its sensitivity to $CO_2$-induced warming, other than perhaps that the changes are not very dramatic even for the most sensitive models. This variation in zonal wind shear response among the models contrasts with the situation for SST and tropospheric temperature changes, where the models exhibit much more consistent tropical climate change signals (i.e., substantial sea surface warming, enhanced upper-tropospheric warming, and enhanced tropospheric moisture content).

## 6. Discussion and conclusions

The results presented in section 4 indicate that the basic findings—more intense simulated hurricanes and greater storm-core precipitation rates in high-$CO_2$ environments—are not strongly dependent on the global climate model used to derive the $CO_2$-induced changes, nor on the particular convective parameterization used in the hurricane model. This suggests that these findings are robust, at least in the context of our idealized experimental design using the variants of the GFDL hurricane model described here or using current potential intensity theories. Our previous study (Knutson et al. 2001) indicated that our results are robust to the inclusion of ocean coupling beneath the simulated hurricanes. The more intense hurricanes and enhanced storm precipitation rates were correlated with warmer SSTs and higher CAPE in our simulations. The global models simulated greater CAPE in the high-$CO_2$ environments despite the enhanced upper-tropospheric warming in the models.

The idealized framework used here may be thought of as addressing the question of the potential intensity of storms, since we presume the existence of a robust initial vortex and do not allow dynamical influences such as vertical wind shear to interfere with the modeled storm's development. In that sense, our intensity results are analogous to potential intensity theories in terms of their applicability to the probability distribution of future intensities, the latter of which also depends on the future frequency of tropical cyclones. A statistical analysis of historical tropical cyclone intensities (Emanuel 2000) found that once a tropical cyclone reaches hurricane strength, it has a roughly equal probability of reaching any intensity from minimal hurricane intensity up to, but not exceeding, its potential intensity. This suggests that the increased intensities simulated in our idealized experiments may be applicable to both the mean intensity and upper-limit intensity of tropical cyclones in a $CO_2$-warmed environment. Changes in tropical circulation features could alter this assessment, but as shown in section 5, the simulated $CO_2$-induced changes in vertical wind shear are fairly modest, without a clear consensus among the CMIP2+ models as to even the sign of the changes.

An important issue is whether and when any $CO_2$-induced increase of tropical cyclone intensity is likely to be detectable in the observations. The magnitude of the simulated increase in our experiments is about +6% for maximum tropical cyclone surface winds. This change occurs for an idealized climate change scenario consisting of an 80-yr increase of $CO_2$ at 1% $yr^{-1}$ compounded (which produces SST increases ranging from 0.8° to 2.4°C in the tropical storm basins in the CMIP2+ models). The smaller SST changes observed for the past 50 yr in the Tropics (e.g., Knutson et al. 1999) imply that the likely SST-inferred intensity change for the past half century is small, relative to both the limited accuracy of historical records of storm intensity and to the apparently large magnitude of interannual variability of storm intensities in some basins (Landsea et al. 1996; Knutson et al. 2001). This further implies that $CO_2$-induced tropical cyclone intensity changes are unlikely to be detectable in historical observations and will probably not be detectable for decades to come. Related to this issue, SSTs over the North Atlantic tropical storm basin have not exhibited a significant warming trend over the past half century (e.g., Knutson et al. 1999). This is a particularly relevant result since the best long-term records of tropical cyclone intensity are found for this basin. Thus, from the perspective of Atlantic SSTs, there is no expectation of an upward trend in tropical cyclone maximum intensities over the past 50 yr, and none is evident in that basin (Landsea et al. 1996). On the other hand, Gettleman et al. (2002) recently reported that CAPE derived from radiosonde observations at several tropical stations has increased significantly in recent decades due to a combination of increased near-surface temperature and water vapor. For example, they found that CAPE at Barbados in the Atlantic tropical storm basin has increased at a rate of 13% *per decade* in recent decades. Also, regarding tropical storm basins other than the NW Atlantic, Knutson et al. (1999) found evidence for significant SST warming trends (~0.5°C per 50 yr or more) in the NE Pacific and Indian Ocean tropical basins, and Gettleman et al. (2002) reported significant CAPE increases in recent decades in the NW tropical Pacific with mixed signals in the SW tropical Pacific. However, long-term homogeneous records of maximum tropical cyclone intensities are apparently even more problematic for these basins than for the Atlantic (e.g., Srivastava et al. 2000; Landsea 2000). In short, this topic presents a number of issues needing further investigation.

The enhanced near-storm precipitation rates in our high-$CO_2$ simulations are consistent with a conceptual picture of enhanced moisture convergence in tropical

cyclones in a warmer climate due to the greater atmospheric moisture content, augmented by a stronger convergent circulation toward the storm core region. Recent reviews of the issue of changes in precipitation extremes with climate warming are provided in Cubasch et al. (2001), Allen and Ingram (2002), and Trenberth et al. (2003).

The main purpose of the present study has been to assess how sensitive our earlier simulation results (increased hurricane intensities and storm precipitation rates in high-$CO_2$ environments) were to the particular climate model used to provide the large-scale environments or to the details of the hurricane model used to simulate the storms. The results show that while there is some quantitative dependence of the sensitivity on the CMIP2+ model used, nearly every combination of CMIP2+ model, hurricane model convection scheme, and tropical storm basin tested shows an increase in simulated storm intensity and of near-storm precipitation rates. This lends support to the notion that after about a century of climate warming in response to increasing greenhouse gases, the upper limits on tropical cyclone intensity imposed by the thermodynamic environment will be altered in such a way as to allow for tropical cyclones with greater precipitation rates and higher intensity (by roughly half a category in our idealized calculations) than occur in the present climate.

*Acknowledgments.* Support for RET was provided by NOAA/GFDL through Contract EA 133R-03-SE-0327. We thank the CMIP2+ modeling groups listed in Table 1 for making model data available for our project through CMIP; Curt Covey and colleagues at PCMDI/LLNL for managing the CMIP2+ data resource; Dan Schwarzkopf for assistance with the hurricane model radiation codes; and Olivier Pauluis, Joe Sirutis, and two anonymous reviewers for their comments on our manuscript.

## REFERENCES

Allen, M. R., and W. J. Ingram, 2002: Constraints on future changes in climate and the hydrologic cycle. *Nature,* **419,** 224–232.

Bender, M. A., and I. Ginis, 2000: Real-case simulations of hurricane–ocean interaction using a high-resolution coupled model: Effects on hurricane intensity. *Mon. Wea. Rev.,* **128,** 917–946.

Bengtsson, L., M. Botzet, and M. Esch, 1996: Will greenhouse gas-induced warming over the next 50 years lead to higher frequency and greater intensity of hurricanes? *Tellus,* **48A,** 57–73.

Broccoli, A., and S. Manabe, 1990: Can existing climate models be used to study anthropogenic changes in tropical cyclone climate? *Geophys. Res. Lett.,* **17,** 1917–1920.

Camp, J. P., and M. T. Montgomery, 2001: Hurricane maximum intensity: Past and present. *Mon. Wea. Rev.,* **129,** 1704–1717.

Cubasch, U., and Coauthors, 2001: Projections of future climate change. *Climate Change 2001: The Scientific Basis,* J. T. Houghton et al., Eds., Cambridge University Press, 525–582.

DeMaria, M., and J. Kaplan, 1994: A Statistical Hurricane Intensity Prediction Scheme (SHIPS) for the Atlantic basin. *Wea. Forecasting,* **9,** 209–220.

Emanuel, K. A., 1986: An air–sea interaction theory for tropical cyclones. Part I: Steady-state maintenance. *J. Atmos. Sci.,* **43,** 585–604.

——, 1987: The dependence of hurricane intensity on climate. *Nature,* **326,** 483–485.

——, 1988: The maximum intensity of hurricanes. *J. Atmos. Sci.,* **45,** 1143–1155.

——, 1991: A scheme for representing cumulus convection in large-scale models. *J. Atmos. Sci.,* **48,** 2313–2335.

——, 1995: Sensitivity of tropical cyclones to surface exchange coefficients and a revised steady-state model incorporating eye dynamics. *J. Atmos. Sci.,* **52,** 3969–3976.

——, 1999: Thermodynamic control of hurricane intensity. *Nature,* **401,** 665–669.

——, 2000: A statistical analysis of tropical cyclone intensity. *Mon. Wea. Rev.,* **128,** 1139–1152.

——, and M. Žiivković-Rothman, 1999: Development and evaluation of a convection scheme for use in climate models. *J. Atmos. Sci.,* **56,** 1766–1782.

Gettelman, A., D. J. Seidel, M. C. Wheeler, and R. J. Ross, 2002: Multidecadal trends in tropical convective available potential energy. *J. Geophys. Res.,* **107,** 4606, doi:10.1029/2001JD001082.

Ginis, I., 1995: Ocean response to tropical cyclones. Global perspectives on tropical cyclones, R. L. Elsberry, Ed., WMO Tech. Doc. TCP-38, World Meteorological Organization, Geneva, Switzerland, 198–260.

Giorgi, F., and Coauthors, 2001: Regional climate information—Evaluation and projections. *Climate Change 2001: The Scientific Basis,* J. T. Houghton et al., Eds., Cambridge University Press, 583–638.

Goldenberg, S. B., and L. J. Shapiro, 1996: Physical mechanisms for the association of El Niño and West African rainfall with Atlantic major hurricane activity. *J. Climate,* **9,** 1169–1187.

——, C. W. Landsea, A. M. Mesta-Nuñez, and W. M. Gray, 2001: The recent increase in Atlantic hurricane activity: Causes and implications. *Science,* **293,** 474–479.

Gray, W. M., 1968: Global view of the origin of tropical disturbances and storms. *Mon. Wea. Rev.,* **96,** 669–700.

——, 1975: Tropical cyclone genesis. Dept. of Atmospheric Science Paper No. 234, Colorado State University, Fort Collins, CO, 121 pp.

Haarsma, R. J., J. F. B. Mitchell, and C. A. Senior, 1993: Tropical disturbances in a GCM. *Climate Dyn.,* **8,** 247–257.

Hansen, J., and Coauthors, 2002: Climate forcings in Goddard Institute for Space Studies SI2000 simulations. *J. Geophys. Res.,* **107,** 4347, doi:10.1029/2001JD001143.

Henderson-Sellers, A., and Coauthors, 1998: Tropical cyclones and global climate change: A post-IPCC assessment. *Bull. Amer. Meteor. Soc.,* **79,** 19–38.

Holland, G. J., 1997: The maximum potential intensity of tropical cyclones. *J. Atmos. Sci.,* **54,** 2519–2541.

Hong, S.-Y., and H.-L. Pan, 1996: Nonlocal boundary layer vertical diffusion in a medium-range forecast model. *Mon. Wea. Rev.,* **124,** 2322–2339.

Houghton, J. T., Y. Ding, D. J. Griggs, M. Noguer, P. J. van der Linden, X. Dai, K. Maskell, and C. A. Johnson, Eds., 2001: *Climate Change 2001: The Scientific Basis.* Cambridge University Press, 881 pp.

Kalnay, E., and Coauthors, 1996: The NCEP/NCAR 40-Year Reanalysis Project. *Bull. Amer. Meteor. Soc.,* **77,** 437–471.

Knutson, T. R., and R. E. Tuleya, 1999: Increased hurricane intensities with $CO_2$-induced warming as simulated using the GFDL hurricane prediction system. *Climate Dyn.,* **15,** 503–519.

——, ——, and Y. Kurihara, 1998: Simulated increase of hurricane intensities in a $CO_2$-warmed climate. *Science,* **279,** 1018–1020.

——, T. L. Delworth, K. W. Dixon, and R. J. Stouffer, 1999: Model assessment of regional surface temperature trends (1949–1997). *J. Geophys. Res.,* **104** (D24), 30 981–30 996.

——, R. E. Tuleya, W. Shen, and I. Ginis, 2001: Impact of $CO_2$-induced warming on hurricane intensities as simulated in a hurricane model with ocean coupling. *J. Climate,* **14,** 2458–2468.

Krishnamurti, T. N., R. Correa-Torres, M. Latif, and G. Daughenbaugh, 1998: The impact of current and possibly future sea surface temperature anomalies on the frequency of Atlantic hurricanes. *Tellus,* **50A,** 186–210.

Kurihara, Y., and R. E. Tuleya, 1981: A numerical simulation study on the genesis of a tropical storm. *Mon. Wea. Rev.,* **109,** 1629–1653.

——, M. A. Bender, and R. J. Ross, 1993: An initialization scheme of hurricane models by vortex specification. *Mon. Wea. Rev.,* **121,** 2030–2045.

——, R. E. Tuleya, and M. A. Bender, 1998: The GFDL hurricane prediction system and its performance in the 1995 hurricane season. *Mon. Wea. Rev.,* **126,** 1306–1322.

Landsea, C. W., 2000: Climate variability of tropical cyclones—Past, present and future. *Storms,* R. Pielke Sr. and R. Pielke Jr., Eds., Vol. 1, Routledge, 221–241.

——, N. Nicholls, W. M. Gray, and L. A. Avila, 1996: Downward trends in the frequency of intense Atlantic hurricanes during the past five decades. *Geophys. Res. Lett.,* **23,** 1697–1700.

Manabe, S., R. J. Stouffer, M. J. Spelman, and K. Bryan, 1991: Transient responses of a coupled ocean–atmosphere model to gradual changes of atmospheric $CO_2$. Part I: Annual mean response. *J. Climate,* **4,** 785–818.

McAvaney, B. J., and Coauthors, 2001: Model evaluation. *Climate Change 2001: The Scientific Basis,* J. T. Houghton et al., Eds., Cambridge University Press, 471–523.

McBride, J. L., and R. Zehr, 1981: Observational analysis of tropical cyclone formation. Part II: Comparison of non-developing versus developing systems. *J. Atmos. Sci.,* **38,** 1132–1151.

Nguyen, K. C., and K. J. E. Walsh, 2001: Interannual, decadal, and transient greenhouse simulation of tropical cyclone-like vortices in a regional climate model of the South Pacific. *J. Climate,* **14,** 3043–3054.

Pan, H.-L., and W.-S. Wu, 1995: Implementing a mass flux convection parameterization package for the NMC Medium-Range Forecast Model. NMC Office Note 409, 40 pp. [Available from NCEP, 5200 Auth Road, Washington, DC 20233.]

Renno, N. O., and A. P. Ingersoll, 1996: Natural convection as a heat engine: A theory for CAPE. *J. Atmos. Sci.,* **53,** 572–585.

Royer, J.-F., F. Chauvin, B. Timbal, P. Araspin, and D. Grimal, 1998: A GCM study of the impact of greenhouse gas increase on the frequency of occurrence of tropical cyclones. *Climate Change,* **38,** 307–343.

Ryan, B. F., I. G. Watterson, and J. L. Evans, 1992: Tropical cyclone frequencies inferred from Gray's yearly genesis parameter: Validation of GCM tropical climates. *Geophys. Res. Lett.,* **19,** 1831–1834.

Santer, B. D., and Coauthors, 1996: A search for human influences on the thermal structure of the atmosphere. *Nature,* **382,** 39–46.

Schade, L. R., and K. A. Emanuel, 1999: The ocean's effect on the intensity of tropical cyclones: Results from a simple coupled atmosphere–ocean model. *J. Atmos. Sci.,* **56,** 642–651.

Shen, W., R. E. Tuleya, and I. Ginis, 2000: A sensitivity study of the thermodynamic environment on GFDL model hurricane intensity: Implications for global warming. *J. Climate,* **13,** 109–121.

Siegel, S., and N. J. Castellan Jr., 1988: *Nonparametric Statistics for the Behavioral Sciences.* McGraw-Hill, 399 pp.

Srivastava, A. K., K. C. Sinha Ray, and U. S. De, 2000: Trends in the frequency of cyclonic disturbances and their intensification over Indian Seas. *Mausam,* **51,** 113–118.

Stouffer, R. J., 2004: Time scales of climate response. *J. Climate,* **17,** 209–217.

Sugi, M., A. Noda, and N. Sato, 2002: Influence of global warming on tropical cyclone climatology: An experiment with the JMA Global Model. *J. Meteor. Soc. Japan,* **80,** 249–272.

Tett, S. F. B., J. F. B. Mitchell, D. E. Parker, and M. R. Allen, 1996: Human influence on the atmospheric vertical temperature structure: Detection and observations. *Science,* **274,** 1170–1173.

Tonkin, H., G. Holland, C. Landsea, and S. Li, 1997: Tropical cyclones and climate change: A preliminary assessment. *Assessing Climate Change: Results from the Model Evaluation and Consortium for Climate Assessments,* W. Howe and A. Henderson-Sellers, Eds., Taylor and Francis Group, 327–360.

——, ——, N. Holbrook, and A. Henderson-Sellers, 2000: An evaluation of thermodynamic estimates of climatological maximum potential tropical cyclone intensity. *Mon. Wea. Rev.,* **128,** 746–762.

Trenberth, K. E., A. Dai, R. M. Rasmussen, and D. B. Parsons, 2003: The changing character of precipitation. *Bull. Amer. Meteor. Soc.,* **84,** 1205–1217.

Tsutsui, J., 2002: Implications of anthropogenic climate change for tropical cyclone activity: A case study with the NCAR CCM2. *J. Meteor. Soc. Japan,* **80,** 45–65.

Vitart, F., J. L. Anderson, and W. F. Stern, 1999: Impact of large-scale circulation on tropical storm frequency, intensity, and location, simulated by an ensemble of GCM integrations. *J. Climate,* **12,** 3237–3254.

Walsh, K. J. E., and B. F. Ryan, 2000: Tropical cyclone intensity increase near Australia as a result of climate change. *J. Climate,* **13,** 3029–3036.

Yukimoto, S., and A. Noda, 2002: Improvements of the Meteorological Research Institute global ocean–atmosphere coupled GCM (MRI-CGCM2) and its climate sensitivity. CGER's Supercomputer Activity Rep., Vol. 10, National Institute for Environmental Studies, Tsukuba, Japan, 37–44.